Biophysical Chemistry 153 (2010) 43–53

Contents lists available at ScienceDirect

Biophysical Chemistry

journal homepage: http://www.elsevier.com/locate/biophyschem

Self-organization of G-quadruplex structures in the hTERT core promoter stabilized by polyaminic side chain perylene derivatives

Emanuela Micheli [a,b], Matteo Martufi [a], Stefano Cacchione [a], Pasquale De Santis [b], Maria Savino [a,*]

[a] Dipartimento di Biologia e Biotecnologie, "Sapienza" Università di Roma, P.le Aldo Moro 5, 00185, Roma, Italy
[b] Dipartimento di Chimica, "Sapienza" Università di Roma, P.le Aldo Moro 5, 00185, Roma, Italy

ARTICLE INFO

Article history:
Received 15 September 2010
Received in revised form 5 October 2010
Accepted 5 October 2010
Available online 13 October 2010

Keywords:
G-quadruplex
Telomerase
hTERT promoter
Perylene derivatives
Induced circular dichroism (ICD)

ABSTRACT

hTERT core promoter regulates telomerase transcription in human cells, thus its structural features are of large interest. We have found that the G-rich hTERT core promoter region, corresponding to the major DNase I hypersensitive site in chromatin organization, contains nine putative G-quadruplex forming sequences (PQS) and is unfavorable for nucleosome formation. Here we show that four PQS are effectively able to form stable parallel intramolecular G-quadruplexes, using PAGE and CD spectroscopy analysis. The PQS-region, as a whole, appears to be organized in three self-interacting G-quadruplexes, probably giving rise to a helicoidal superstructure, as shown by CD and polymerase stop assay.
POL–HPDI drugs, that we previously found useful in selectively stabilizing telomeric G-quadruplex, are able to stabilize both the single intramolecular G-quadruplex and the PQS-region superstructure. The features of their induced CD spectra suggest that POL–HPDIs bind to single G-quadruplexes and to whole PQS-region superstructure, mainly by end-stacking interactions.

1. Introduction

Nucleic acid sequences, containing tracts of 3–4 consecutive guanines, have the potential to fold into four stranded structures, called G-quadruplexes. G-quadruplexes arise from the stacking of G-quartets, planar associations of four guanines held together by Hoogsteen hydrogen bonds, and are stabilized by the coordination of monovalent cations in the central cavity of the G-quartets [1].

The possible role of G-quadruplex structures in the regulation of basic biological processes, such as transcription and replication, is still a matter of debate. In eukaryotes, the highest concentration of DNA sequences with the potential to form G-quadruplexes is located at telomeres, the nucleoproteic structures that protect the ends of eukaryotic chromosomes. Telomeres consist of tandem arrays of short sequences containing three or four guanines (TTAGGG in mammals), ending in a 3′ single-stranded G-rich overhang that is extended by the reverse-transcriptase enzyme telomerase. *In vitro*, the G-rich 3′-overhang is able to spontaneously form intramolecular G-quadruplex structures at physiological K^+ concentrations [2,3]. Importantly, the formation *in vivo* of G-quadruplexes at telomeres has been experimentally shown in ciliates such as *Stylonichia* and very recently G-quadruplex sequences have been shown to be evolutionary conserved in *Saccharomyces cerevisiae* [4,5]. G-quadruplex formation is thought to interfere with telomerase elongation. Since telomerase activity is essential to guarantee unlimited proliferative ability to most cancer cells, the research for G-quadruplex-stabilizing ligands has become an attractive anti-cancer strategy [6,7]. We have previously shown that polyaminic side chains–hydrosoluble perylene diimides (POL–HPDIs), synthesized in our research group, dramatically increase the human telomeric G-quadruplex thermodynamic stability, have a significant selectivity for G-quadruplex structure with respect to duplex structure of genomic DNA, and are able to inhibit telomerase *in vitro* [8–10].

Recently, genome-wide analyses have shown that sequences with the potential to form G-quadruplex structures (PQS, putative G-quadruplex sequences) are widespread both in prokaryotic and in eukaryotic genomes [11]. Interestingly, PQS frequency is higher in functionally important regions. In humans, over 40% of gene promoters contain at least one PQS. In particular, G-quadruplex structures have been characterized in cancer related gene promoters [12], such as c-MYC, VEGF, HIF-1α, Ret, KRAS, Bcl-2, c-Kit, PDGF-A and c-Myb, suggesting that G-quadruplexes may play a role in gene regulation. It was also shown that the G-quadruplex formed within the promoter region of c-MYC can be stabilized by a small molecule in living cells, which results in transcriptional repression of c-MYC [13], suggesting that this approach could represent a practicable way to modulate gene expression. The presence of DNA sequences able to form G-quadruplex structures *in vitro* has been recently shown in the

* Corresponding author. Tel.: +39 0649912238; fax: +39 064440812.
E-mail address: maria.savino@uniroma1.it (M. Savino).

0301-4622/$ – see front matter © 2010 Elsevier B.V. All rights reserved.
doi:10.1016/j.bpc.2010.10.003

promoter of the hTERT gene, coding the catalytic subunit of human telomerase [14–16]. Targeting the activity of this gene could represent a useful strategy to counteract cancer cell proliferation [17,18], since telomerase activity in cancer cells mainly depends on hTERT reactivation [19]. In the last few years we have studied the structural features of the hTERT core promoter from −100 to +1 upstream of the ATG site, where a polypurinic/polypyrimidinic stretch can be a target for triple helix as well as give rise to superstructures, deriving from intermolecular G-quadruplexes [20,21].

In this paper we report the structural characterization and the thermodynamic stability of the putative G-quadruplex structures in the human telomerase core promoter. Adopting the *quadparser* method [11], we have found that the hTERT promoter between −400 to +1 contains twelve consecutive G-tracts, which constitute nine partially overlapped sequences with the potentiality to form G-quadruplexes. We have selected the four more stable single G-quadruplex structures on the basis of polyacrylamide gel electrophoresis and circular dichroism spectroscopy of model oligonucleotides. In the whole G-rich region, we have found that some of them self-interact, giving rise to a probably helicoidal superstructure. Furthermore, we report that their interactions with three polyaminic side chains–hydrosoluble perylene diimides (POL–HPDIs) result in a significant stabilization of the single G-quadruplex as well as of their self-organization on the whole hTERT promoter.

2. Materials and methods

2.1. Oligonucleotides

DNA oligonucleotides were purchased by MWG-Biotech. The sequences of the oligonucleotides are shown in Table 1. All oligonucleotides were HPLC purified and checked by denaturing PAGE. Their concentrations were determined by the absorbance at 260 nm using a spectrophotometer.

2.2. Polyacrylamide gel electrophoresis (PAGE)

The samples (10 μM oligonucleotides in TE buffer, Tris–HCl 10 mM pH 7.6, and EDTA 1 mM) were heated to 95 °C for 10 min; then annealed by slowly cooling to room temperature in the presence of 100 mM KCl or NaCl or LiCl. After an incubation at 4 °C overnight, the samples were run on 18% native PAGE (19:1 acrylamide:bisacrylamide ratio) with TBE as electrophoretic run buffer, containing the same salt concentration of the run samples. Each run was performed at room temperature for about 1 h and 30 min at 100 V. The oligonucleotide bands were detected by fluorescence. The gels were stained with SYBR Green I Nucleic acids dye (purchased by SIGMA) and scanned using the Typhoon 9200 (Amersham Biosciences).

2.3. Circular dichroism (CD)

CD spectra were recorded on a JASCO J-715 spectropolarimeter equipped with a thermostatted cell holder, using a quartz cell of 1 cm optical path length and an instrument scanning speed of 100 nm/min, with a response time of 1 s. The samples were prepared as described for PAGE experiments; the oligonucleotides were dissolved in TE buffer, and where appropriate, the samples also contained different concentrations of KCl. The CD data represent three averaged scans and all CD spectra are baseline-corrected for signal contribution due to the buffer. The spectra were calculated with J-700 Standard Analysis software (Japan Spectroscopic Co., Ltd) and are reported as molar ellipticity versus wavelength; the molar ellipticity was computed considering the oligonucleotide concentration as strand concentration. The spectra were recorded at 25 °C, except for the melting studies in which the temperature ranges from 25 °C to 90 °C.

For the induced circular dichroism (ICD) spectra, the ratio [DNA]/[POL–HPDI] has been chosen equal to 4, on the basis of the results previously reported [9], considering POL–HPDI concentration in molecules (20 μM) and the DNA concentration in nucleotides (80 μM). The samples were prepared in TE buffer in the presence of 5 mM KCl and the spectra were recorded as described above.

2.4. DNA polymerase stop assay

The 5′-end-labeled HT-primer (80 nM) and HT-template (160 nM) in a Tris–HCl buffer (10 mM, pH 7.6) were annealed by heating at 95 °C for 10 min and slowly cooling down to room temperature. After adding KCl and drugs at the appropriate concentrations, the samples were incubated for 2 h at 30 °C and then stored at 4 °C overnight.

The primer extension reaction was initiated by adding dNTPs (final concentration 100 μM), 3.75 U/reaction of DNA polymerase, Klenow fragment (Fermentas) or DreamTaq™ DNA polymerase (Fermentas), and the corresponding reaction buffer, that in the first case contains 50 mM Tris–HCl (pH 8.0), 5 mM $MgCl_2$ and 1 mM DTT, while in the latter case is the DreamTaq™ Buffer. The reaction was performed for 30 min at 37 °C for Klenow fragment and at 65 °C for the DreamTaq™ DNA polymerase, and then stopped adding 150% of stop buffer (10 mM EDTA, 10 mM NaOH, 0.1% xylene cyanole, and 0.1% bromophenol blue in formamide solution) heating at 95 °C for 10 min. Finally, the samples were analyzed on a 10% denaturing polyacrylamide gel (19:1 acrylamide:bisacrylamide ratio) and 8 M

Table 1
Sequences (5′ to 3′) of the oligonucleotides, model of the hTERT promoter PQS, used in our studies.

HT1	GGGGAGGGGCTGGGAGGG	HT*[a]	AA-[HT1]-CC
HT2	GGGGCTGGGAGGGCCCGGAGGGGG	HT2*	GA-[HT2]-CT
HT3	GGGAGGGCCCGGAGGGGGCTGGG	HT3*	CT-[HT3]-CC
HT4	GGGCCCGGAGGGGGCTGGGCCGGGG	HT4*	GA-[HT4]-AC
HT5	GGGGGCTGGGCCGGGACCCGGG	HT5*	GA-[HT5]-AG
HT6	GGGCCGGGGACCCGGGAGGGG	HT6*	CT-[HT6]-TC
HT7	GGGGACCCGGGAGGGGTCGGG	HT7*	CC-[HT7]-AC
HT8	GGGAGGGGTCGGGACGGGG	HT8*	CC-[HT8]-CG
HT9	GGGGTCGGGACGGGGCGGGG	HT9*	GA-[HT9]-TC
HT_{68}	GGGGAGGGGCTGGGAGGGCCCGGAGGGGGCTGGCCGGGGACCCGGGAGGGGTCGGGACGGGGCGGGG		
HT^*_{72}	AA-[HT_{68}]-TC		
HT-template	GGAAAGGAAGGGGAGGGGCTGGGAGGGCCCGGAGGGGGCTGGGCCGGGGACCCGGGAGGGGTCGGGACGGGGCGGGGTCCGCGCGGAGGAGGC–GGAGCTGGAAGGTGAAG		
HT-primer[b]	CTTCACCTTCCAGCTCCG		
HT-template (−PQS1)	GGGGCGGGGCAGGGCTGGGGAGGGCCCAGGGGCCGGGTCGGGGGTCCGCGCGGAGGAGGCGGAGCTGGAAGGTGAAG		

[a] The asterisks indicate the sequences including two flanking bases at the two ends.
[b] HT-primer is the primer used in the DNA polymerase stop assay.

urea, run at 50 W for about 3 h. Then the gel was dried, exposed to a Storage Phosphor Screen and acquired using the Typhoon 9200 (Amersham Biosciences).

2.5. Statistical mechanics modeling of nucleosome positioning

Few years ago, we advanced a theoretical method, based on sequence-dependent DNA curvature and flexibility, which allows the quantitative prediction of the free energy of nucleosome formation in terms of thermodynamics and structural parameters of the dinucleotide steps [22,23].

The model is based on the sequence-dependent curvature of the DNA chain, which regulates the free energy required to transform recurrent DNA tracts along the sequence in a nucleosomal shape.

Statistical mechanics allows the calculation of the elastic free energy difference in the nucleosome competitive reconstitution and consequently, the thermodynamic affinity, $\Delta G_{el}(k)$, of a DNA segment, L (148 bp):

$$\beta\Delta G_{el}(k) = \beta\Delta E^{o}_{el}(k) + Z(k) - \ln(J_0(iZ(k))) - \frac{3}{2}L\ln\left(\frac{b(k)}{b}\right) \quad (1)$$

where $\Delta E_{el}{}^{\circ}(k)$ is the first-order elastic energy required to distort the kth tract of L bp in the nucleosomal form.

$$\Delta E^{o}_{el}(k) = \frac{b(k)}{2L}\left(A_n(\mu) - A^{o}_{f}(\mu)\right)^2 + \frac{t(k)}{2}(2\pi\Delta Tw_k(k))^2 \quad (2)$$

where the first term which represents the bending energy contribution, is conveniently expressed on the basis of Parseval [24] equality in terms of the differences between the Fourier transform amplitudes of the curvature function, $A_n(\mu)$ and $A^{o}_{f}(\mu)$, with frequency $\mu = -0.18$; $b(k)$ is the apparent bending force constant relative to the kth DNA tract. $\Delta Tw(k)$ is the change of twisting number of the kth free DNA tract after transformation into the nucleosomal structure and $t(k)$ the apparent torsional force constant.

The last three terms of Eq. (1) represent the entropy contribution to the relative thermodynamic stability of a nucleosome on the kth position. $Z(k) = -\frac{\beta b(k) A_n(\mu) A^{o}_{f}(\mu)}{L}$ and $J_0(iZ(k))$ are the zero-order Bessel function of the imaginary argument $iZ(k)$. $A_n(\mu)A^{o}_{f}(\mu)$ is the product of the Fourier amplitudes of the curvature function of nucleosomal and free DNA and represents the modulus of the correlation between the superstructure of the nucleosomal DNA as found in the crystal structure [25] and that of the free form according to the convolution theorem. $b(k)/b^*$ which represents the relative rigidity of the kth nucleosomal DNA with respect to the standard one, was assumed to be equivalent to T/T^*, the normalized dinucleotide empirical melting temperature of the kth DNA tract.

The theoretical free energy values so obtained, showed satisfactory agreement with the experimental data for a number of DNAs, but major deviations for others. This agreement, however, was strictly correlated ($R = 0.99$) with the free DNA effective curvature, $\langle A_f \rangle$, which represents in modulus and phase the degree of similarity of the free DNA curvature with that of the nucleosome. This strongly indicated the existence of an additional curvature-dependent contribution to the free energy, which appears to destabilize the nucleosome. Such a contribution was obtained by fitting the free energy deviations by a function of the effective curvature [22,23]. We interpreted this free energy contribution as due to the groove contractions in intrinsically curved free DNAs, which stabilize the water spine and counterion interactions adding a further energy cost to the nucleosome formation. This contribution can be neglected for straight and slightly curved sequences.

If we calculate the free energy minima along a DNA sequence, long enough to accommodate more than one nucleosome, we can assume that the minima along the sequence represent virtual nucleosome positions. In fact, more recently, the model was adopted with success in predicting the nucleosome positioning of genomes [26].

3. Results

3.1. The hTERT promoter contains nine putative G-quadruplex sequences (PQS) in a region with low propensity to form nucleosomes

The potentiality to form G-quadruplexes has been evaluated in the hTERT promoter, in the 400-nt region upstream of the ATG site (Fig. 1A), by means of the bioinformatic method *quadparser*, recently developed by Huppert and coll. [11]. The *quadparser* algorithm searches for sequences of the form $d(G_{3+}N_{1-7}G_{3+}N_{1-7}G_{3+}N_{1-7}G_{3+})$, where N refers to any base. The segment of hTERT promoter between −167 and −100 is guanine rich and shows a high content of putative G-quadruplex sequences (PQS). This 68-nt long segment (PQS-region) contains twelve stretches of three or more guanines (G-tracts), with linkers ranging in length from 1 to 5 nt; thus it is possible to identify nine partially overlapped sequences following the folding rule defining a PQS.

It has been recently shown that hTERT transcription is associated with the presence of a major deoxyribonuclease (DNase I) hypersensitive site positioned nearby the hTERT transcription start site [27], probably corresponding to a nucleosome-free region. Since nucleosome stability and G-quadruplex formation seem to be inversely correlated [28], we have adopted the chromatin organization of the hTERT core promoter as further constrain to provide evidence for G-quadruplex formation. We analyzed the nucleosome positioning in the hTERT promoter region from −400 to +1 taking advantage of the theoretical method, developed in our research group (a short account is reported in the section Materials and methods) [26], which derives the sequence-dependent free energy of nucleosome formation by sequence-dependent DNA curvature and flexibility. The obtained profile of theoretical nucleosome positioning is reported in Fig. 1B. The G-rich region containing the PQS (−167/−100) and corresponding to the major DNase-hypersensitive site in the hTERT promoter [27] is characterized by a high energy cost to form nucleosomes.

3.2. Six PQS are able to form secondary structures, ascribable to G-quadruplex formation

Since it has been reported that the flanking sequences at 3′- and 5′-end are important for the G-quadruplex folding and stability [29,30], to investigate the propensity of the nine identified PQS in the hTERT promoter to fold in a G-quadruplex structure, we used two series of model oligonucleotides, reported in Table 1. The first series, indicated as HT (from 1 to 9), corresponds to the nine PQS with terminal guanine bases; the oligonucleotides of second series (HT* in Table 1) include also the two flanking basis both at the 5′- and at the 3′-end in the promoter.

In order to study the G-quadruplex formation, we studied the mobility of HT and HT* oligonucleotides by polyacrylamide gel electrophoresis (PAGE). It is well known that the formation of monomolecular G-quadruplex increases the electrophoretic mobility of human telomeric DNA with respect to that of the corresponding not structured telomeric DNA [31]. The cations' role, namely the specificity of K^+ ions in stabilizing G-quadruplex, as compared to Li^+ ions, strongly supports that the increase of electrophoretic mobility is due to the formation of a “bona fide” intramolecular G-quadruplex [32], which is characterized by a high friction coefficient due to its compactness.

We screened the nine oligonucleotides pairs, HT and HT* (see Table 1), by PAGE in TE buffer by varying the added 100 mM monovalent cation (K^+, Na^+, and Li^+). The obtained results are reported in Fig. 2. Surprisingly, in the presence of KCl (Fig. 2A), four oligonucleotides, HT1, HT2, HT8 and HT9, show a mobility much

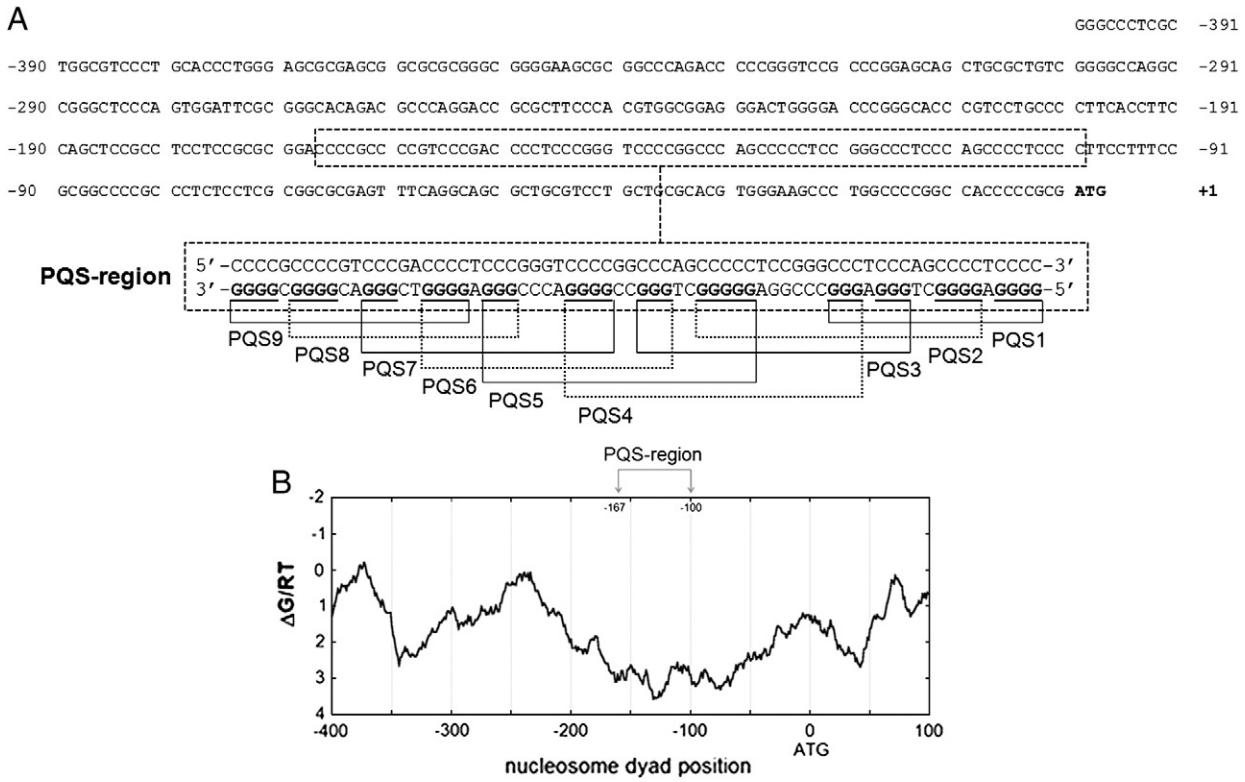

Fig. 1. (A) Sequence of the hTERT promoter in the 400-nt region upstream of the ATG site. The PQS-region containing the nine putative quadruplex sequences (PQS) is highlighted in the inset. (B) Free energy of nucleosome positioning along the −400/+100 region of hTERT promoter as function of nucleosome dyad position.

lower than that of a marker (lane "M" in the figure), namely an 18-nt long unstructured oligonucleotide. On the contrary, two oligonucleotides, HT4 and HT6, migrate faster than the marker. The remaining three HT show mobility similar to that of the marker or slightly lower. In Fig. 2A, we have also reported the electrophoresis of HT*, that are all characterized by an increase of molecular weight, due to the two nucleotides added at each end: their behavior, different from that of HT, seems to be correlated with their molecular weight. The decrease of the four HT mobility can be attributed either to the formation of multimers of intramolecular G-quadruplexes or to the formation of intermolecular G-quadruplexes; the different behavior of HT* strongly favors the first possibility [21].

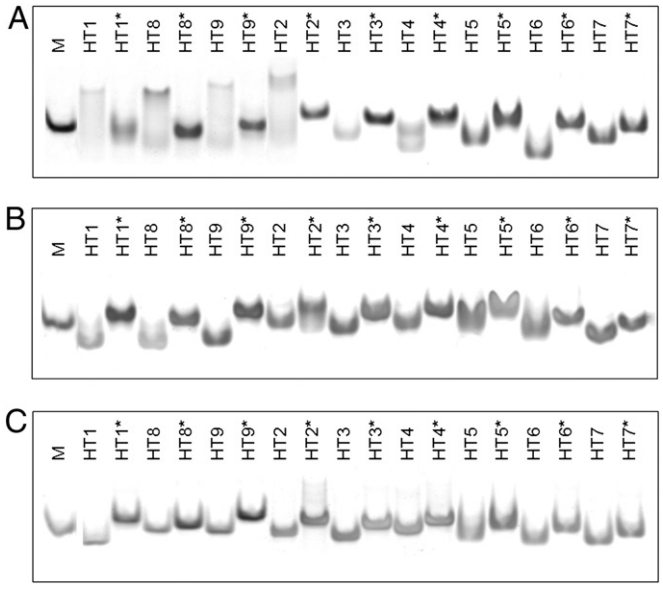

Fig. 2. A typical polyacrylamide gel electrophoresis of HT and HT* oligonucleotides in TE buffer plus 100 mM KCl (A), or 100 mM NaCl (B), or 100 mM LiCl (C). "M" indicates an 18-mer oligonucleotide, which is unstructured in the adopted experimental conditions.

The formation of multimers is supported by the increase of HT mobility, in 100 mM NaCl, as shown in Fig. 2B. In these conditions, HT1, HT8 and HT9, show the canonical increase of electrophoretic mobility associated with the formation of monomolecular G-quadruplex. The other HT show mobility similar with those of HT*, that are dependent on their molecular weight.

Potassium and sodium dependence of the four HT (HT1, HT2, HT8 and HT9) mobility is confirmed by PAGE in the presence of LiCl (Fig. 2C), since in this conditions both HT and HT* are characterized by mobility depending on their molecular weight, showing that G-quadruplex structures are not formed.

To sum up, PAGE indicates that in the presence of 100 mM KCl or NaCl six PQS are able to form folded structures, presumably G-quadruplex; more in detail, a monomolecular structure is formed by three sequences, HT1, HT8, and HT9 in NaCl and by HT4 and HT6 in KCl; a multimerization process is observed for HT1, HT2, HT8 and HT9 in the presence of KCl. Three sequences, HT3, HT5 and HT7 do not seem able to fold as G-quadruplex in the same conditions. Also the nine HT* seem not able to form G-quadruplex, at least considering their electrophoretic behavior.

3.3. Selection of four PQS that fold in predominantly parallel G-quadruplex structures

CD is a very useful technique in G-quadruplex characterization. The dependence of the CD spectrum features on KCl concentration is a clear sign for G-quadruplex formation; moreover CD allows assigning tentatively the topology of the structure, although NMR spectroscopy and/or X-ray crystallography are necessary to definitively solve the G-quadruplex structure. In most cases, parallel G-

quadruplexes exhibit a high positive band at 260 nm and a negative band at 240 nm. Antiparallel quadruplex species show a characteristic positive band at 290 nm, and a negative band at 260 nm [33]. However, it is worth considering that one should be cautious in the interpretation of G-quadruplex topology, based only on CD spectra, since multiple G-quadruplex conformations (parallel, antiparallel, (3 + 1)) could be present [16,34,35].

We have measured the spectra of all HT either in TE buffer or in TE buffer plus 100 mM KCl. In the presence of KCl, HT1, HT2, HT8 and HT9 show CD spectrum features typical of G-quadruplex formation (Fig. 3A), namely a high positive band at 262 nm, a small positive band, or in some cases a shoulder, at 295 nm and a negative band at 240 nm. These features suggest the existence of a predominant parallel quadruplex population, along with a small antiparallel population or the presence of (3 + 1) G-quadruplex. On the contrary, the HT4 and HT6 CD spectra (Fig. S1) change only slightly in the presence of KCl, indicating a low amount of G-quadruplex, in good agreement with the PAGE results. However, it is worth noting that the decrease of the intensity ratio between the band at 262 nm and the band at 295 nm suggests a higher fraction of antiparallel population. The CD spectra of the other three HT (Fig. S1) are characterized by significantly lower ellipticities with respect to the first four HT. These features indicate a very low ability to form a G-quadruplex structure.

The CD spectra recorded for the HT* (Fig. 3B) are characterized by the same spectra features as those of the HT, except that their molar ellipticities are significantly lower; e.g. HT8* CD is characterized by an ellipticity at 262 nm that is one third of that of HT8. We suggest that the higher ellipticity of HT, with respect to HT*, derive from multimers asymmetric self-organization (see also the section Discussion).

In conclusion, on the basis of PAGE and CD analyses, four sequences out of nine, PQS1, PQS2, PQS8 and PQS9, appear able to fold as stable monomolecular G-quadruplex, predominantly with a parallel topology. Since the four screened sequences are partially overlapped (see Fig. 1A), the study of the whole PQS-region, by means of the oligonucleotides HT_{68} and HT^{*}_{72} (see Table 1), is necessary to establish the sequences among the four PQS that are effectively involved in the organization of the structure of the full-length promoter fragment, between −167 and −100.

3.4. Presence of two G-quadruplexes and their ability to induce the folding of a third one in the PQS-region

To study the structure of the full-length PQS-region we used CD spectroscopy and a biochemical method, namely the DNA polymerase stop assay. Both methods allow us to study the structure of the whole hTERT promoter DNA fragment. The CD spectrum of HT_{68}, the 68-mer oligonucleotide representing the full-length PQS-region (see Table 1), was recorded in TE buffer with and without 100 mM KCl; the obtained results are reported in Fig. 4A. As in the case of the truncated HT, the spectra features of HT_{68} are potassium-dependent and are characterized by a high positive band at 262 nm, a small shoulder at 288 nm and a negative band at 237 nm, indicating a mixed parallel/antiparallel G-quadruplex topology, with prevalence of the parallel one. The presence of the two flanking bases on the HT^{*}_{72} sequence does not sensibly influence CD spectrum features (data not shown). It is worth noting that the molar ellipticities are about fourfold higher than those corresponding to the single HT* sequences (compare Figs. 3A and 4A). Since the molar ellipticity was computed considering the concentration in molecules of the oligonucleotide, the comparison between the HT_{68} spectra and those of HT and HT* permits to gain structural information on the whole DNA fragment. The obtained ellipticity values are larger than those corresponding to the sum of the CD spectra of two independent HT*-quadruplexes, suggesting an additional contribution due to a third G-quadruplex or to the presence of a G-quadruplex self-interaction.

A powerful assay to gain sound information on the structures present on the whole fragment is the DNA polymerase stop assay [36]. Namely, if the DNA template is capable of forming any secondary structures, such as a G-quadruplex, the elongation of the DNA polymerase will be arrested during primer extension, due to enzyme inability to bypass the secondary structures. Therefore we designed a DNA template containing the 12 G-tracts of the PQS-region (called HT-template, whose sequence is reported in Table 1) and studied its capacity to form intramolecular G-quadruplex by DNA polymerase stop assay (Fig. 4B). The obtained results show that, in the absence of KCl or in the presence of 100 mM NaCl, there is no arrest of DNA synthesis along the fragment. In the presence of KCl (ranging from 5

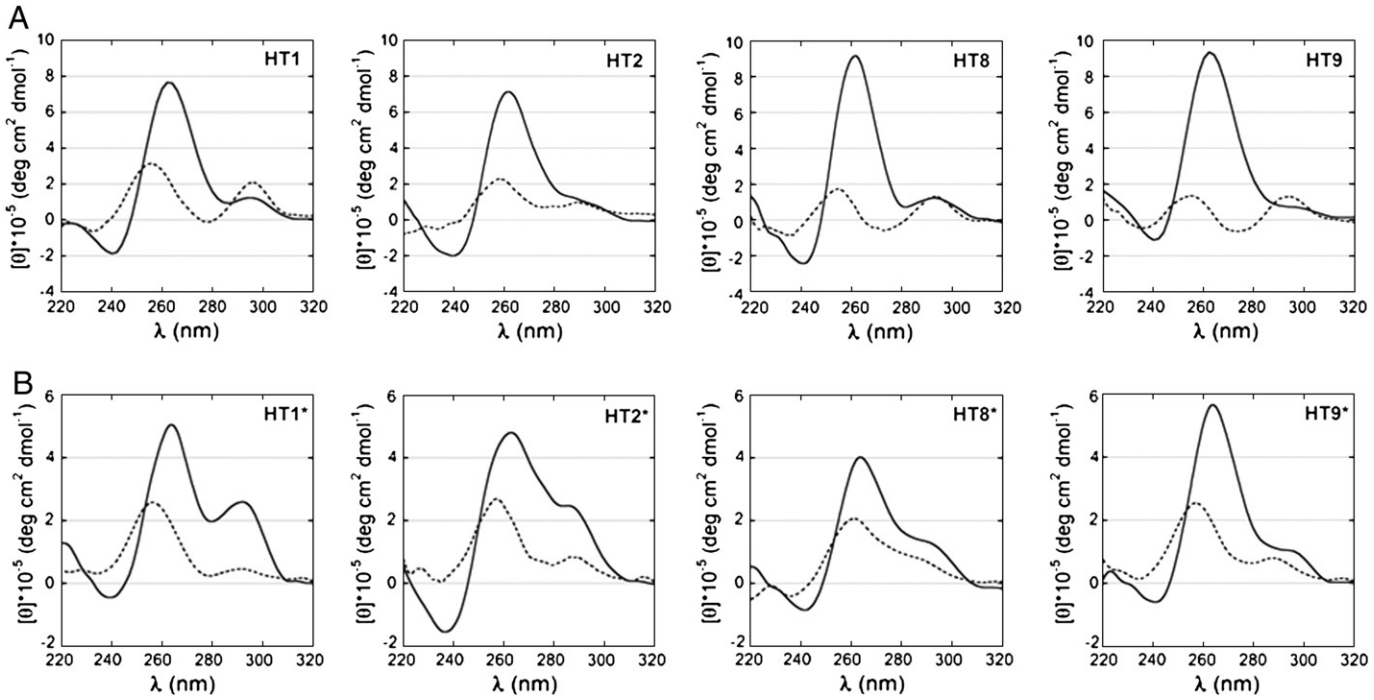

Fig. 3. Circular dichroism (CD) spectra of four HT and HT*. The spectra were measured in TE buffer in the absence (dashed lines) and in the presence (solid lines) of 100 mM KCl.

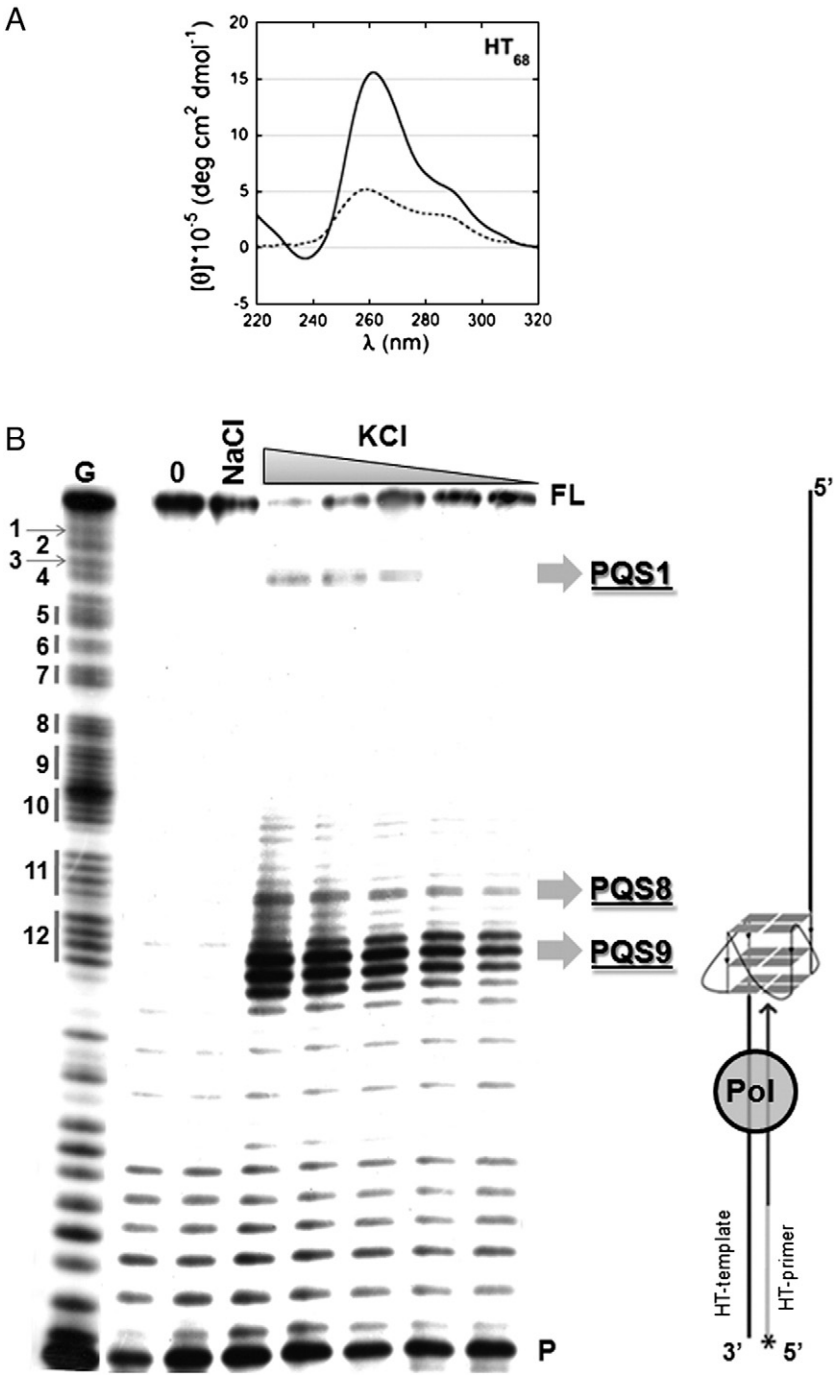

Fig. 4. Study of the structural organization of the whole PQS-region in the hTERT promoter by CD spectroscopy and polymerase stop assay. (A) CD spectra of HT_{68} in TE buffer in the absence (dashed line) and in the presence (solid line) of 100 mM KCl. (B) DNA polymerase stop assay on HT-template in the presence of decreasing concentrations of KCl (respectively 100, 50, 20, 10 and 5 mM). For the sake of comparison also the samples in TE buffer (lane 0) and in TE buffer plus 100 mM NaCl (lane NaCl) are reported. To the left of the gel the G sequencing is reported as the first lane and the numbers of the G-tracts are also shown. The primer (P) and the full-length product (FL) bands and the stop sites corresponding to PQS9, PQS8 and PQS1 are shown to the right of the gel.

to 100 mM), a significant amount of arrested synthesis products appears, depending on potassium concentration. In order to determine the exact point in which DNA polymerase stops, the template was sequenced by Sanger (dideoxy) method (reported in the first electrophoresis lane). A major DNA polymerase arrest can be seen in correspondence of the 3′-end of G-tract no. 12, indicating the formation of a G-quadruplex structure, that should involve PQS9, starting from this position. Minor stops corresponding to G-tracts no. 11 and 4, suggest the formation of PQS8 and PQS1 G-quadruplexes but with a frequency significantly lower than that of PQS9. It is worth noting that the DNA polymerase stop assay allows putting in evidence only the first stop that the enzyme encounters on its path.

To obtain information on the structure of the whole PQS-region, we carried out the assay also on a modified model template, able to establish the presence of intermediate G-quadruplex structures. In Fig. 5A the rationale of our scheme is illustrated. If the low stability PQS5-quadruplex is stabilized by the presence of PQS9, a stop at PQS5 level should be found. Fig. 5B clearly shows a strong stop at PQS5, whose intensity is directly dependent on KCl concentration, indicating that PQS9-quadruplex stabilizes the G-quadruplex formed by PQS5.

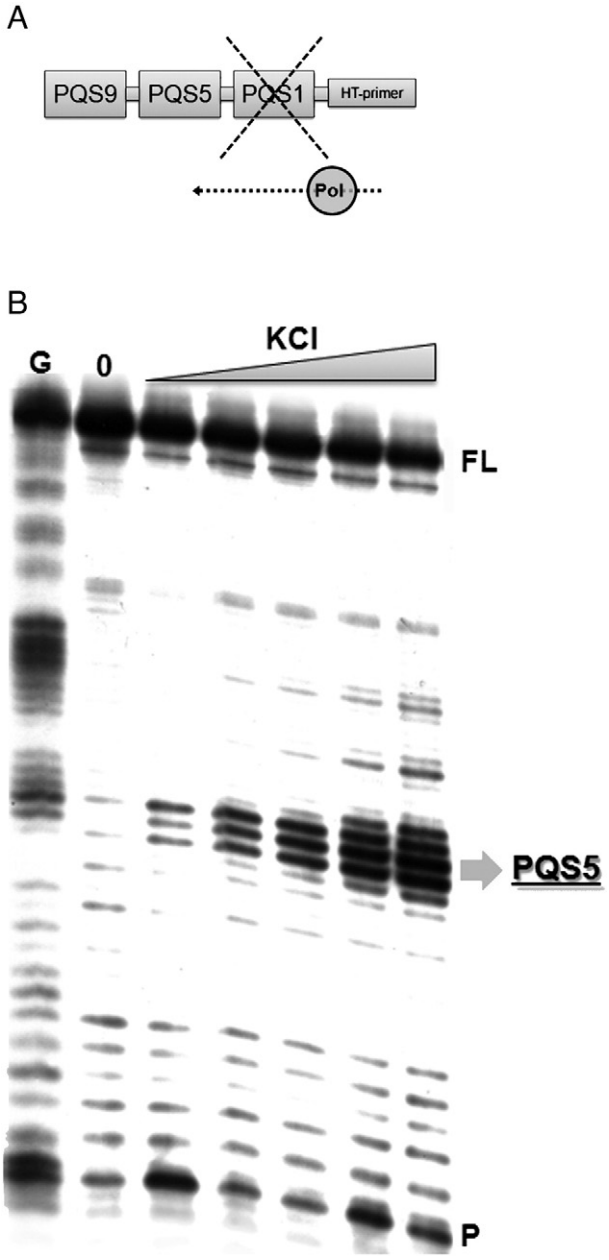

Fig. 5. (A) Schematic illustration of the model oligonucleotide HT-template (−PQS1) used in the DNA polymerase stop assay. The HT-template has been modified, removing the sequence corresponding to PQS1 and inverting the strand direction. (B) DNA polymerase stop assay on HT-template in the presence of decreasing concentrations of KCl (respectively 100, 50, 20, 10 and 5 mM). For the sake of comparison also the sample in TE buffer is reported. In the first lane the G sequencing is reported. The primer (P) and the full-length product (FL) bands and the stop sites corresponding to PQS5 are shown to the right of the gel.

The ability of a G-quadruplex structure to stop the DNA polymerase path should be connected with its thermodynamic stability. In order to investigate the stability of the PQS-quadruplexes, highlighted by DNA polymerase stop assay, we measured the thermal melting profiles of the corresponding HT and HT*, recording the CD spectra of the oligonucleotides at increasing temperature, in the presence of 5 mM KCl. The melting profiles and the melting temperatures are reported in Fig. 6. It is worth noting that, for all the considered sequences, the melting temperature of HT* is about 5–12 °C lower than that of the corresponding HT. The higher stability of HT with respect to HT* suggests a stabilization effect, provided by a multimerization process. It is tempting to consider that a similar effect could be present in the whole promoter fragment, although limited to the stabilizing interactions between two or three G-quadruplexes.

3.5. Polyaminic side chains–hydrosoluble perylene diimides (POL–HPDIs) are able to bind and stabilize the G-quadruplex structures in the hTERT promoter

An interesting question is whether PQS in the hTERT promoter could be the target of G-quadruplex stabilizing agents that could alter hTERT expression. We approached this issue by studying the ability of three POL–HPDIs (POLyaminic side chains–Hydrosoluble Perylene DiImides) to interact with the hTERT promoter G-quadruplexes. These molecules belong to a series of perylene derivatives with two polyaminic side chains, synthesized in our research group, which we found able to selectively stabilize human telomeric G-quadruplex and inhibit telomerase in a cell free system [8,9].

A DNA polymerase stop assay was carried out in the presence of increasing concentration of three POL–HPDIs, POL-3, POL-4 and POL-8, whose chemical structures are reported in Fig. 7. Low KCl concentration (5 mM) and high temperature (65 °C) of DNA synthesis represent stringent conditions to assay the influence of the three POL–HPDIs. In fact, in 5 mM KCl the main stops due to the G-quadruplex formation are present in a very limited number of HT_{68} molecules. Fig. 8B shows that the full-length product decreases with the increase of POL–HPDI concentration in all cases, whereas the intensity of the first polymerase stop, corresponding to PQS9, increases. The PQS9 stop increase is similar in the case of POL-3 and POL-8, and lower in the case of POL-4. The densitometric profiles, reported in Fig. 8B, reveal other two stops, corresponding to PQS3 and PQS4, suggesting that the presence of the drugs, especially POL-3, could stabilize less stable G-quadruplexes, more efficiently than K^+ ions.

The intensity of the full-length and the primer bands was quantified and the obtained trends are reported in Fig. 8C. At higher concentration POL-3 and POL-8 are able to stabilize also the primer/template adduct, represented by the primer band; this indicates an affinity of the two drugs also for duplex DNA. POL-4 appears more selective since the full-length product decreases, without increase of the primer/template.

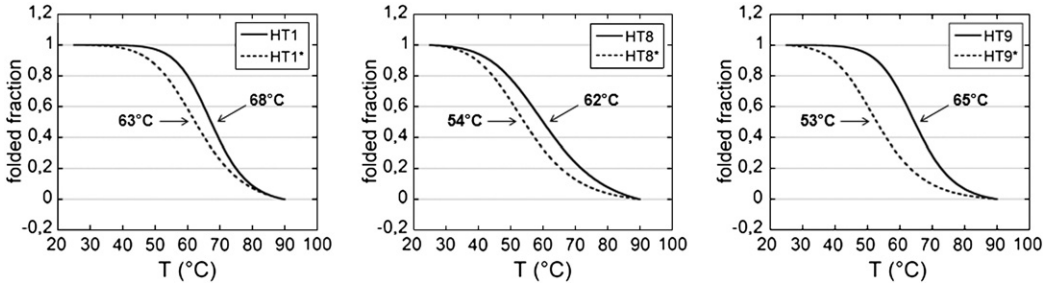

Fig. 6. CD melting profiles of HT1, HT8 and HT9 (solid lines) and HT1*, HT8* and HT9* (dashed lines). The arrows indicate the melting temperature (T_m), as the temperature corresponding to a folded fraction equal to 0.5.

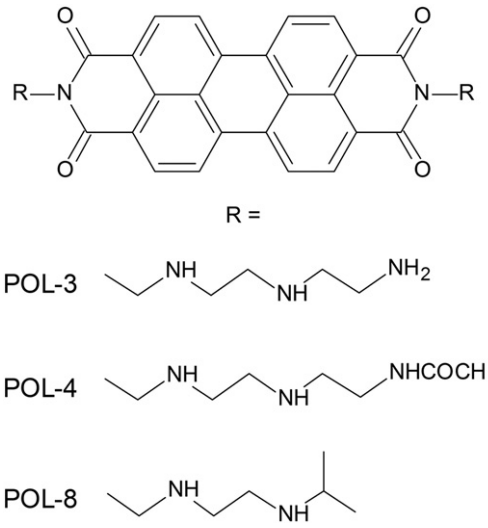

Fig. 7. Chemical structure of the three polyaminic side chains–perylene diimides (POL–HPDIs). The perylene diimide moiety and the three different side chains are illustrated.

To investigate drug stabilization effect, we carried out a CD melting assay of the HT_{68} in 5 mM KCl solution in the presence of the three different POL–HPDIs (Fig. 9). At room temperature drug binding seems to slightly favor the formation of an antiparallel G-quadruplex in all cases, suggested by the small decrease of the band at 262 nm and the correspondent increase of the shoulder intensity at 290 nm (Fig. 9), with respect to the CD spectra of HT_{68} without drugs. Increasing the temperature the antiparallel structure melts, whereas the parallel one seems stable also at 90 °C upon POL–HPDI binding. The stabilization of the parallel G-quadruplex structure at high temperatures is greater in the case of POL-8 and less evident in the case of POL-3 and POL-4 (POL-8>POL-3>POL-4).

3.6. End-stacking of POL–HPDIs on the hTERT G-quadruplex structures

POL–HPDIs are symmetrical molecules, therefore they are not optically active. Since G-quadruplex DNA structures have a CD spectrum only in the wavelength range 220–320 nm, the CD spectra of DNA–drug complexes, recorded in the wavelength range 350–700 nm, are exclusively due to the ligand bound to DNA and thus asymmetrically perturbed. The CD spectra of the three POL–HPDIs in the presence of the HT-quadruplexes were analyzed in the wavelength range 350–700 nm to obtain information on the molecular features of the interactions between the drugs and the G-quadruplex structures. The features of the induced CD (ICD) spectra of the complexes between POL-3, POL-8 and POL-4 and G-quadruplex structure (Fig. 10) are directly correlated with the absorption spectra as reported in Supplementary Material (Fig. S2).

The comparison of the ICD spectra of the different POL–HPDI in the presence of HT1, HT8 and HT9, and the respective HT*, in the range 350–700 nm, shows that POL-3 and POL-8 have a similar behavior and both give rise to ICD spectra characterized by higher ellipticities than POL-4. ICD spectra are characterized by a major positive band at about 550 and a minor one at 510 nm, not so evident in the case of POL-4; in some cases a low shoulder at 475 nm is also present. The similarity of the CD spectra with the absorption ones (see Fig. S2) suggests that the POL–HPDIs are strongly coupled with the terminal G-quartet of HT G-quadruplex, interacting in a monomeric form, as indicated by the non-conservative spectra. This finding is consistent with the perylene moiety end-stacking on the terminal G-quartet [9].

Comparing the CD spectra of the HPDIs recorded with HT or HT* sequences, it is worth noting that the ellipticity values are higher in the case of all HT* with respect to the corresponding HT.

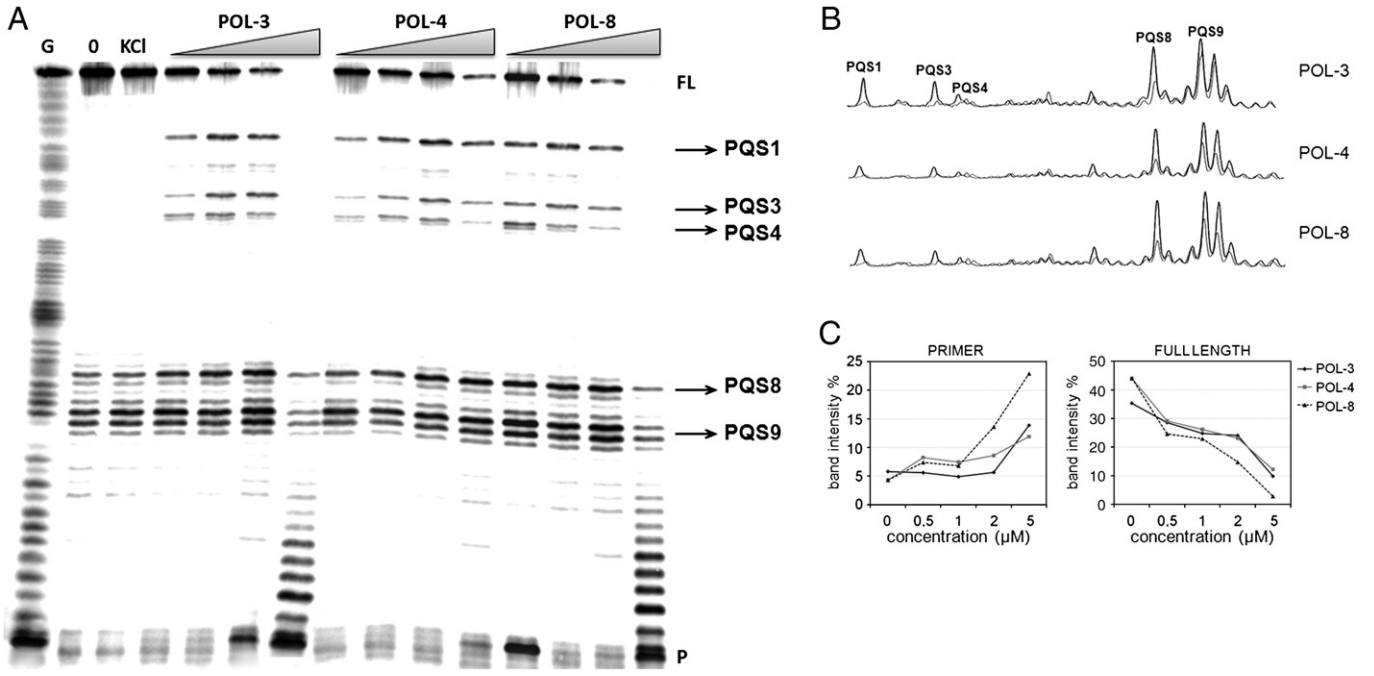

Fig. 8. Characterization of G-quadruplex formation in the PQS-region of the hTERT promoter in the presence of the three POL–HPDIs (POL-3, POL-4 and POL-8). (A) DNA polymerase stop assay performed in 5 mM KCl in the presence of increasing POL–HPDI concentration (0.5, 1, 2 and 5 μM). For the sake of comparison also the samples in TE buffer (lane 0) and in TE buffer plus 5 mM KCl (lane KCl) are reported. In the first lane to the left of the gel the G sequencing is reported. The primer (P) and the full-length product (FL) bands and the stop sites corresponding to PQS9, PQS8, PQS4, PQS3 and PQS1 are shown to the right of the gel. (B) Densitometric profiles of the lanes corresponding to 2 μM POL–HPDI (solid lines). For each drug the comparison with the lane KCl is reported (dashed lines). (C) Quantification of the bands of the full-length product and the primer for the three POL–HPDIs plotted against drug concentrations. The percentage was computed as related to the total band intensity.

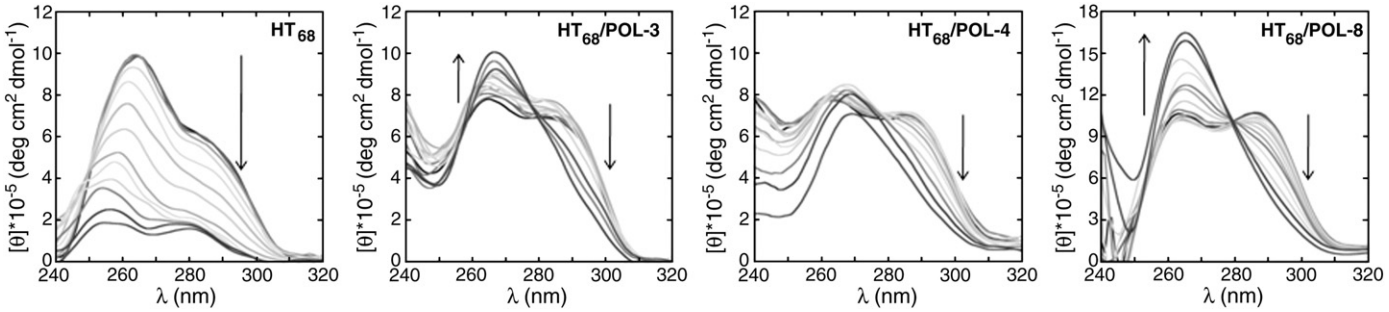

Fig. 9. CD spectra of HT_{68} in TE buffer with 5 mM KCl, measured at increasing temperature, in the range 25–90 °C with an increasing step of 5 °C. The same CD spectra were recorded in the presence of 5 μM POL-3, POL-4 and POL-8, from the left to the right of the panel. Arrows indicate the increasing temperature.

The spectra of the three molecules in the presence of HT_{68} are reported in Fig. 8 and show molar ellipticities comparable to those obtained with the truncated sequences HT.

4. Discussion

The hTERT promoter region from −400 to the +1 contains nine consecutive putative G-quadruplex forming sequences, PQS (see Fig. 1), whose biological significance is indicated by the fact that they coincide with major DNase I hypersensitive sites, found in promoter chromatin organization [27]. Taking into account that chromatin hypersensitive sites often coincide with modified or less stable nucleosomes [37], we derived the nucleosome positioning along the hTERT promoter by theoretical analysis of DNA sequence-dependent curvature and flexibility [26]. We found that the PQS-region shows a strikingly low propensity to form nucleosomes as shown in Fig. 1B. Thus, it is tempting to suggest that the presence of PQS and unfavorable nucleosome positioning could be coupled also in other gene promoters. Very recently a similar correlation was proposed on the basis of human genome bioinformatic analysis [28,38].

The presence of G-quadruplexes in hTERT core promoter, their structural features and their stabilization by polyaminic perylene derivatives, POL–HPDIs, recently synthesized and studied in our research group [8,9], have been investigated in this paper.

We selected among the nine PQS the four sequences PQS1, PQS2, PQS8 and PQS9 (see Fig. 1A), that are able to fold in predominantly parallel intramolecular G-quadruplex structures in the presence of potassium ions, by native PAGE and CD spectroscopy; similar results were recently obtained by Hurley and coll. [15] and by Phan and coll. [16]. In the latter paper, it was shown, by NMR analysis, that PQS1 can adopt also a (3 + 1) G-quadruplex conformation, whose amount is significantly lower than that of parallel G-quadruplex.

The reduced electrophoretic mobility of HT1, HT2, HT8 and HT9 model oligonucleotides in 100 mM KCl (Fig. 2A) is ascribable to the formation of G-quadruplex multimers due to stacking interactions between the terminal G-quartet of two adjacent monomolecular G-quadruplexes; on the contrary, this interaction seems hindered in the case of the corresponding HT* by the dangling terminals (see Table 1). This consideration is strongly supported by the comparison of the CD spectra of HT and HT* (Fig. 3). The ellipticity values of HT CD spectra are significantly higher than those of HT*, suggesting that interactions between single G-quadruplexes give rise to an asymmetric, probably helicoidal, superstructure. The increase of molar ellipticities of HT with respect to HT*, affects in particular the band at about 265 nm,

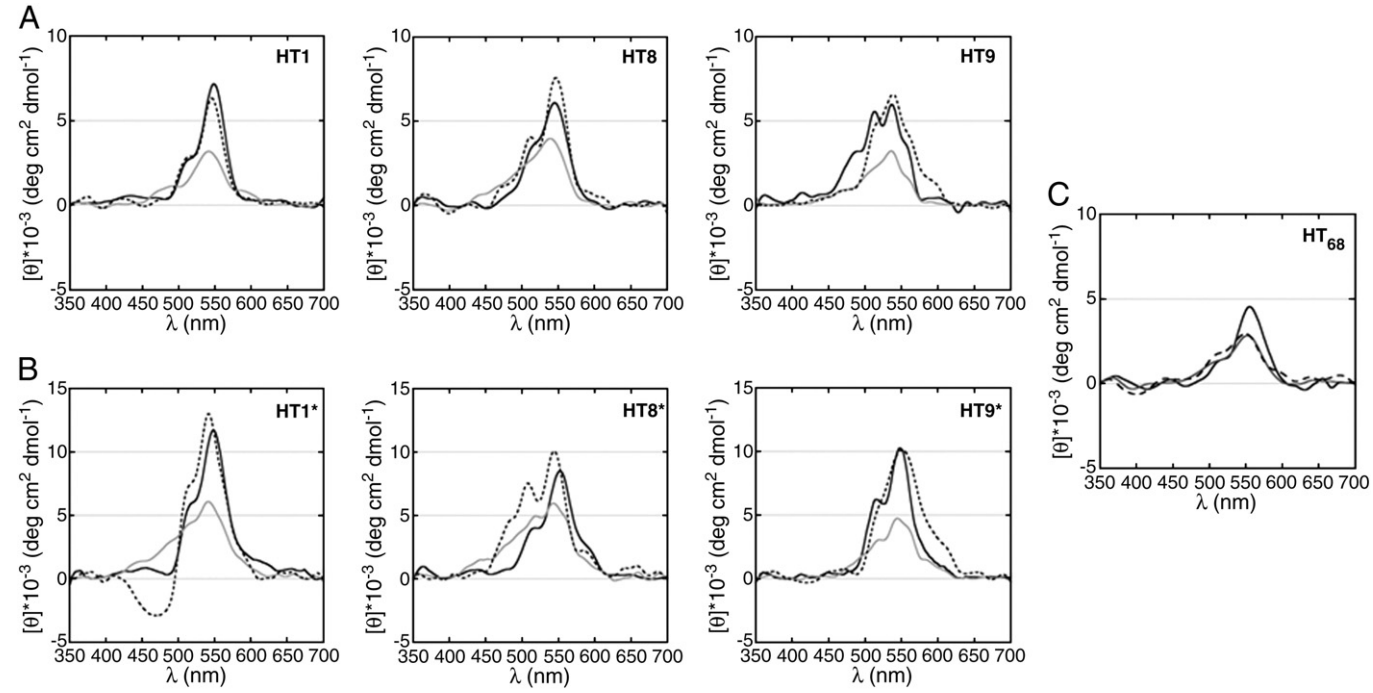

Fig. 10. Induced CD spectra of POL-3 (black line), POL-4 (gray line) and POL-8 (dashed line) in the presence of HT1, HT8 and HT9 (A), of the corresponding HT* (B) and of HT_{68}, the model oligonucleotide for the whole PQS-region (C). The ICD spectra were measured in the perylene chromophore wavelength range (350–700 nm), where the HPDI ellipticities are equal to zero, in the absence of G-quadruplex perturbation.

related to the parallel topology, while the band at 290 nm corresponding to the antiparallel one appears to be unaffected or even decreased. This observation suggests that the multimerization process involves mainly the parallel G-quadruplex structures, in agreement with previously reported results [39]. For the same reason, HT4 and HT6, whose CD spectra indicate a high antiparallel fraction (see Fig. S1), are not able to form multimers; only one band, corresponding to the monomolecular G-quadruplex, is shown in PAGE in the presence of KCl (see Fig. 2A).

The study of HT_{68}, i.e. the whole PQS-region of hTERT promoter containing the nine partially overlapped PQS, appears necessary to clarify the structural organization of the whole promoter region. A DNA polymerase stop assay was performed at increasing KCl concentration in order to confirm the formation of G-quadruplex in the PQS-region. Since the three HT corresponding to the polymerase stops, namely HT1, HT8 and HT9, have similar melting temperatures (see Fig. 6), we suggest that the presence of one major stop (at HT9) and two minor stops (at HT8 and HT1) is probably due to the occurrence of a dynamic conformational equilibrium between the different G-quadruplex structures. The DNA polymerase, starting from the 3′ side of HT-template, firstly has to run into the secondary structure formed at HT9. Thus, it is reasonable to consider that the stop at HT9 does not exclude the simultaneous presence of the G-quadruplex at HT1 on the same template molecule.

On this basis, it can be proposed that the PQS-region folds simultaneously in two G-quadruplex structures, namely PQS1 and PQS9. However, the molar ellipticities HT_{68} are higher than those predictable considering the formation of only two G-quadruplexes. The obtained values suggest the presence of a further asymmetrical contribution on HT_{68} CD, that could be either the interaction between PQS1 and PQS9 or the presence of a third G-quadruplex in the sequence included between PQS1 and PQS9. The polymerase stop assay of the modified HT-template, lacking PQS1 (see Fig. 5), supports strongly the second possibility, since the enzyme stops at PQS5, because of the formation of a G-quadruplex structure, stabilized by the presence of the PQS9-quadruplex. Thus, we propose a model based on the presence in the PQS-region of three adjacent G-quadruplexes, formed by PQS1, PQS9 and PQS5, interacting each other by the stacking of their terminal G-quartets. This interaction could provide a stabilization effect for PQS5-quadruplex, not detectable from the reported studies of the isolated HT5.

Several studies have recently reported that G-quadruplex ligands can modulate gene transcription by stabilizing the G-quadruplex formation within their core promoter [40,41]; for this reason, the binding of three POL–HPDIs to the hTERT G-quadruplex, previously studied by us as telomeric G-quadruplex ligands and telomerase inhibitors [8–10], appears of interest. The ICD spectra of POL-3, POL-4 and POL-8, measured in the presence of the HT, show the effective capability of these molecules to bind to monomolecular G-quadruplex mainly by ligands end-stacking on the terminal G-quartet [8,9].

The comparison between the CD spectra of POL–HPDI complex with HT and those with the corresponding HT*, further supports the formation of HT multimers, because of reduced ICD ellipticities, deriving from a lower number of binding sites available for the ligand, due to the HT-multimerization process. A reduction of free binding sites can be suggested also in the case of the complexes of HPDIs with the HT_{68}, based on stacking interactions between the three different G-quadruplexes, formed by PQS1, PQS5 and PQS9; this finding represents a further support to our model.

Furthermore, the CD melting studies of the whole PQS-region (HT_{68}) in the presence of POL–HPDIs (see Fig. 10) show that the binding of these molecules leads to the stabilization of the overall structure, that lasts in a folded form even at high temperatures.

The reported findings strongly suggest that hTERT promoter superstructure, based on monomeric G-quadruplex interactions, should be more significant than single monomeric G-quadruplex in regulating telomerase gene transcription. The superstructure role could be enforced by small organic molecules, such as POL–HPDIs, capable to stabilize G-quadruplex self-interactions.

Supplementary data to this article can be found online at doi:10.1016/j.bpc.2010.10.003.

Acknowledgments

This research has been financially supported by MIUR-PRIN 2007 and by Istituto Pasteur–Fondazione Cenci Bolognetti. Thanks are due to Marco Franceschin for making available the three POL–HPDI molecules.

References

[1] S. Burge, G.N. Parkinson, P. Hazel, A.K. Todd, S. Neidle, Quadruplex DNA: sequence, topology and structure, Nucleic Acids Res. 34 (2006) 5402–5415.
[2] S. Neidle, Human telomeric G-quadruplex: the current status of telomeric G-quadruplexes as therapeutic targets in human cancer, FEBS J. 277 (2010) 1118–1125.
[3] A.T. Phan, Human telomeric G-quadruplex: structures of DNA and RNA sequences, FEBS J. 277 (2010) 1107–1117.
[4] H.J. Lipps, D. Rhodes, G-quadruplex structures: *in vivo* evidence and function, Trends Cell Biol. 19 (2009) 414–422.
[5] J.A. Capra, K. Paeschke, M. Singh, V.A. Zakian, G-quadruplex DNA sequences are evolutionarily conserved and associated with distinct genomic features in *Saccharomyces cerevisiae*, PLoS Comput. Biol. 6 (2010) e1000861.
[6] J.H. Tan, L.Q. Gu, J.Y. Wu, Design of selective G-quadruplex ligands as potential anticancer agents, Mini Rev. Med. Chem. 8 (2008) 1163–1178.
[7] J. Cuesta, M.A. Read, S. Neidle, The design of G-quadruplex ligands as telomerase inhibitors, Mini Rev. Med. Chem. 3 (2003) 11–21.
[8] M. Franceschin, C.M. Lombardo, E. Pascucci, D. D'Ambrosio, E. Micheli, A. Bianco, G. Ortaggi, M. Savino, The number and distances of positive charges of polyamine side chains in a series of perylene diimides significantly influence their ability to induce G-quadruplex structures and inhibit human telomerase, Bioorg. Med. Chem. 16 (2008) 2292–2304.
[9] E. Micheli, C.M. Lombardo, D. D'Ambrosio, M. Franceschin, S. Neidle, M. Savino, Selective G-quadruplex ligands: the significant role of side chain charge density in a series of perylene derivatives, Bioorg. Med. Chem. Lett. 19 (2009) 3903–3908.
[10] E. Micheli, D. D'Ambrosio, M. Franceschin, M. Savino, Water soluble cationic perylene derivatives as possible telomerase inhibitors: the search for selective G-quadruplex targeting, Mini Rev. Med. Chem. 9 (2009) 1622–1632.
[11] J.L. Huppert, S. Balasubramanian, Prevalence of quadruplexes in the human genome, Nucleic Acids Res. 33 (2005) 2908–2916.
[12] Y. Qin, L.H. Hurley, Structures, folding patterns, and functions of intramolecular DNA G-quadruplexes found in eukaryotic promoter regions, Biochimie 90 (2008) 1149–1171.
[13] A. Siddiqui-Jain, C.L. Grand, D.J. Bearss, L.H. Hurley, Direct evidence for a G-quadruplex in a promoter region and its targeting with a small molecule to repress c-MYC transcription, Proc. Natl Acad. Sci. USA 99 (2002) 11593–11598.
[14] E. Micheli, M. Martufi, M. Savino, Putative intramolecular G-quadruplex structures within a regulatory element of the human telomerase (hTERT) promoter, ESF Conference — Self-assembly of Guanosine Derivatives: From Biological Systems to Nanotechnological Applications, Universitätszentrum Obergurgl, Austria, 2009.
[15] S.L. Palumbo, S.W. Ebbinghaus, L.H. Hurley, Formation of a unique end-to-end stacked pair of G-quadruplexes in the hTERT core promoter with implications for inhibition of telomerase by G-quadruplex-interactive ligands, J. Am. Chem. Soc. 131 (2009) 10878–10891.
[16] K.W. Lim, L. Lacroix, D.J. Yue, J.K. Lim, J.M. Lim, A.T. Phan, Coexistence of two distinct G-quadruplex conformations in the hTERT promoter, J. Am. Chem. Soc. 132 (2010) 12331–12342.
[17] D.R. Corey, Telomeres and telomerase: from discovery to clinical trials, Chem. Biol. 16 (2009) 1219–1223.
[18] M. Folini, C. Brambilla, R. Villa, P. Gandellini, S. Vignati, F. Paduano, M.G. Daidone, N. Zaffaroni, Antisense oligonucleotide-mediated inhibition of hTERT, but not hTERC, induces rapid cell growth decline and apoptosis in the absence of telomere shortening in human prostate cancer cells, Eur. J. Cancer 41 (2005) 624–634.
[19] W.E. Wright, M.A. Piatyszek, W.E. Rainey, W. Byrd, J.W. Shay, Telomerase activity in human germline and embryonic tissues and cells, Dev. Genet. 18 (1996) 173–179.
[20] L. Rossetti, G. D'Isa, C. Mauriello, M. Varra, P. De Santis, L. Mayol, M. Savino, A model for triple helix formation on human telomerase reverse transcriptase (hTERT) promoter and stabilization by specific interactions with the water soluble perylene derivative, DAPER, Biophys. Chem. 129 (2007) 70–81.
[21] S. Pisano, M. Varra, E. Micheli, T. Coppola, P. De Santis, L. Mayol, M. Savino, Superstructural self-assembly of the G-quadruplex structure formed by the homopurine strand in a DNA tract of human telomerase gene promoter, Biophys. Chem. 136 (2008) 159–163.
[22] A. Scipioni, S. Pisano, C. Anselmi, M. Savino, P. De Santis, Dual role of sequence-dependent DNA curvature in nucleosome stability: the critical test of highly bent *Crithidia fasciculata* DNA tract, Biophys. Chem. 107 (2004) 7–17.

[23] C. Anselmi, P. De Santis, R. Paparcone, M. Savino, A. Scipioni, From the sequence to the superstructural properties of DNAs, Biophys. Chem. 95 (2002) 23–47.
[24] M.R. Spiegel, Schaum's Outline of Theory and Problems of Fourier Analysis, with Applications to Boundary Value Problems, McGraw-Hill, New York, 1974.
[25] K. Luger, A.W. Mader, R.K. Richmond, D.F. Sargent, T.J. Richmond, Crystal structure of the nucleosome core particle at 2.8 A resolution, Nature 389 (1997) 251–260.
[26] P. De Santis, S. Morosetti, A. Scipioni, Prediction of nucleosome positioning in genomes: limits and perspectives of physical and bioinformatic approaches, J. Biomol. Struct. Dyn. 27 (2010) 747–764.
[27] S. Wang, J. Zhu, The hTERT gene is embedded in a nuclease-resistant chromatin domain, J. Biol. Chem. 279 (2004) 55401–55410.
[28] H.M. Wong, J.L. Huppert, Stable G-quadruplexes are found outside nucleosome-bound regions, Mol. Biosyst. 5 (2009) 1713–1719.
[29] L. Martino, B. Pagano, I. Fotticchia, S. Neidle, C. Giancola, Shedding light on the interaction between TMPyP4 and human telomeric quadruplexes, J. Phys. Chem. B 113 (2009) 14779–14786.
[30] V. Viglasky, L. Bauer, K. Tluckova, P. Javorsky, Evaluation of human telomeric G-quadruplexes: the influence of overhanging sequences on quadruplex stability and folding, J. Nucleic Acids 2010 (2010).
[31] L. Rossetti, M. Franceschin, A. Bianco, G. Ortaggi, M. Savino, Perylene diimides with different side chains are selective in inducing different G-quadruplex DNA structures and in inhibiting telomerase, Bioorg. Med. Chem. Lett. 12 (2002) 2527–2533.
[32] H. Han, C.L. Cliff, L.H. Hurley, Accelerated assembly of G-quadruplex structures by a small molecule, Biochemistry 38 (1999) 6981–6986.
[33] J. Kypr, I. Kejnovska, D. Renciuk, M. Vorlickova, Circular dichroism and conformational polymorphism of DNA, Nucleic Acids Res. 37 (2009) 1713–1725.
[34] S. Masiero, R. Trotta, S. Pieraccini, S. De Tito, R. Perone, A. Randazzo, G.P. Spada, A non-empirical chromophoric interpretation of CD spectra of DNA G-quadruplex structures, Org. Biomol. Chem. 8 (2010) 2683–2692.
[35] V. Dapic, V. Abdomerovic, R. Marrington, J. Peberdy, A. Rodger, J.O. Trent, P.J. Bates, Biophysical and biological properties of quadruplex oligodeoxyribonucleotides, Nucleic Acids Res. 31 (2003) 2097–2107.
[36] H. Han, L.H. Hurley, M. Salazar, A DNA polymerase stop assay for G-quadruplex-interactive compounds, Nucleic Acids Res. 27 (1999) 537–542.
[37] Y. Mito, J.G. Henikoff, S. Henikoff, Histone replacement marks the boundaries of cis-regulatory domains, Science 315 (2007) 1408–1411.
[38] K. Halder, R. Halder, S. Chowdhury, Genome-wide analysis predicts DNA structural motifs as nucleosome exclusion signals, Mol. Biosyst. 5 (2009) 1703–1712.
[39] N. Smargiasso, F. Rosu, W. Hsia, P. Colson, E.S. Baker, M.T. Bowers, E. De Pauw, V. Gabelica, G-quadruplex DNA assemblies: loop length, cation identity, and multimer formation, J. Am. Chem. Soc. 130 (2008) 10208–10216.
[40] S. Cogoi, L.E. Xodo, G-quadruplex formation within the promoter of the KRAS proto-oncogene and its effect on transcription, Nucleic Acids Res. 34 (2006) 2536–2549.
[41] Y. Qin, E.M. Rezler, V. Gokhale, D. Sun, L.H. Hurley, Characterization of the G-quadruplexes in the duplex nuclease hypersensitive element of the PDGF-A promoter and modulation of PDGF-A promoter activity by TMPyP4, Nucleic Acids Res. 35 (2007) 7698–7713.